Novel fluorophores for localization-based microscopy

Diffraction limit

Diffraction limit

GB Airy, Transactions of the Cambridge Philosophical Society, 1835

Point Spread Function (PSF)

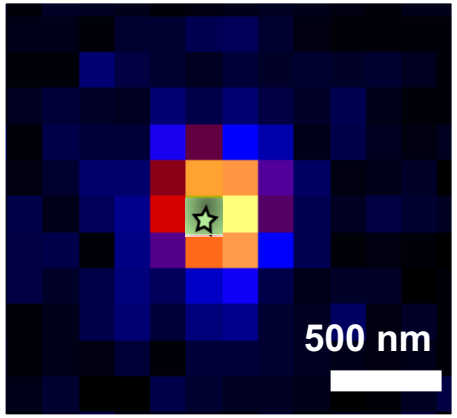

E Abbe, Arch Mikr Anat,1873

$$w_{x,y} \approx \frac{\lambda}{2NA} > 200nm$$

$$w_z \approx \frac{2\lambda\eta}{(NA)^2} > 500nm$$

Diffraction limit

Point Spread Function (PSF)

E Abbe, Arch Mikr Anat,1873

GB Airy, Transactions of the Cambridge Philosophical Society, 1835

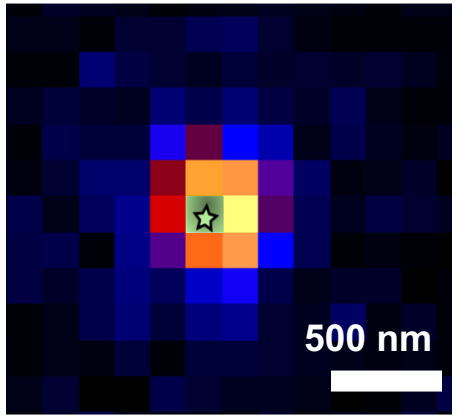

$$w_{x,y} \approx \frac{\lambda}{2NA} > 200nm$$

$$w_z \approx \frac{2\lambda\eta}{(NA)^2} > 500nm$$

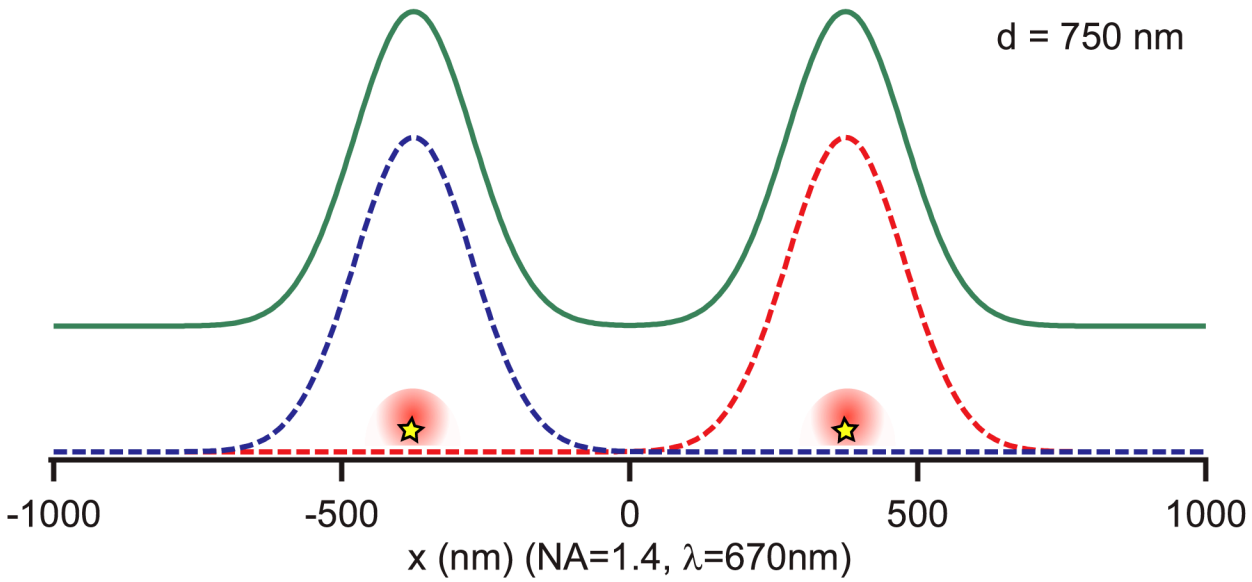

Diffraction limit

Point Spread Function (PSF)

E Abbe, Arch Mikr Anat,1873

GB Airy, Transactions of the Cambridge Philosophical Society, 1835

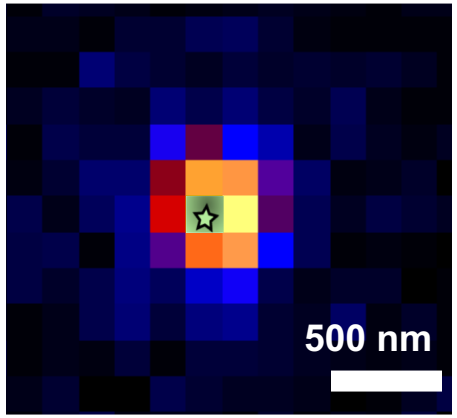

$$w_{x,y} \approx \frac{\lambda}{2NA} > 200nm$$

$$w_z \approx \frac{2\lambda\eta}{(NA)^2} > 500nm$$

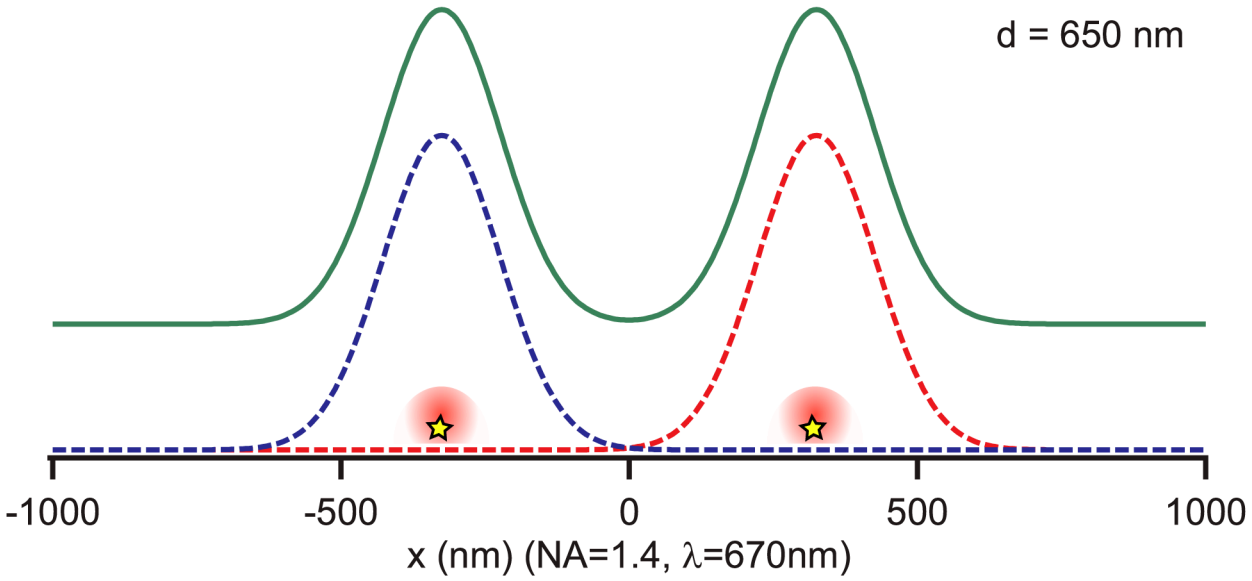

Diffraction limit

Point Spread Function (PSF)

E Abbe, Arch Mikr Anat,1873

GB Airy, Transactions of the Cambridge Philosophical Society, 1835

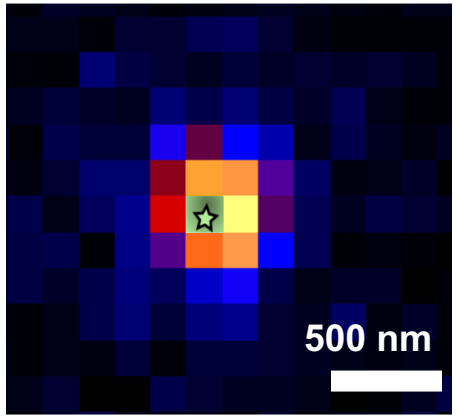

$$w_{x,y} \approx \frac{\lambda}{2NA} > 200nm$$

$$w_z \approx \frac{2\lambda\eta}{(NA)^2} > 500nm$$

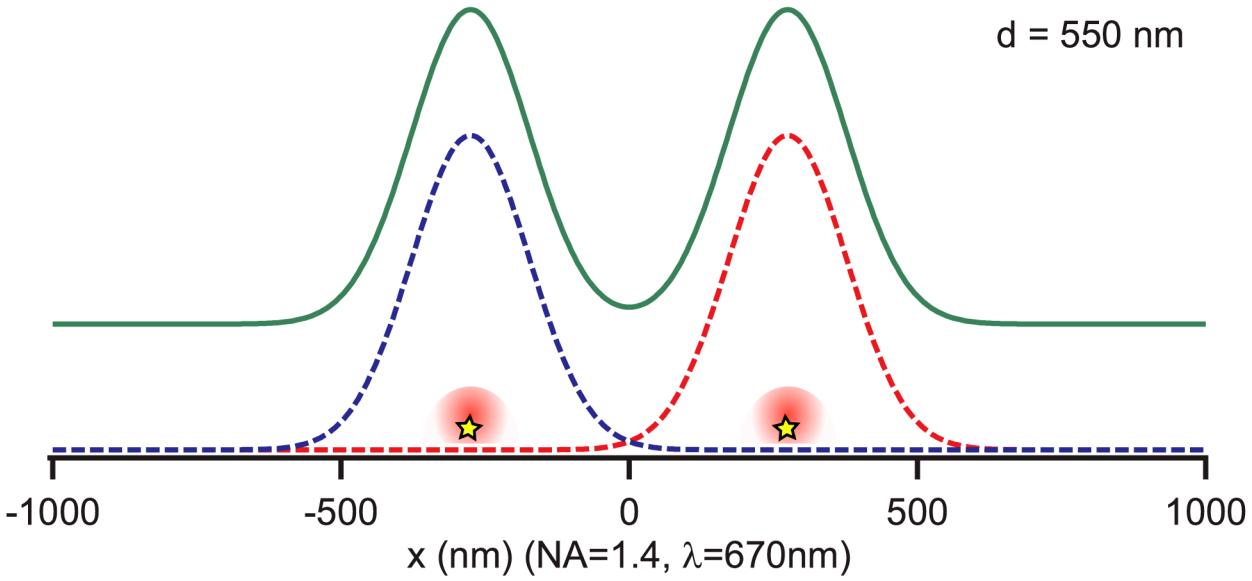

Diffraction limit

Point Spread Function (PSF)

E Abbe, Arch Mikr Anat,1873

GB Airy, Transactions of the Cambridge Philosophical Society, 1835

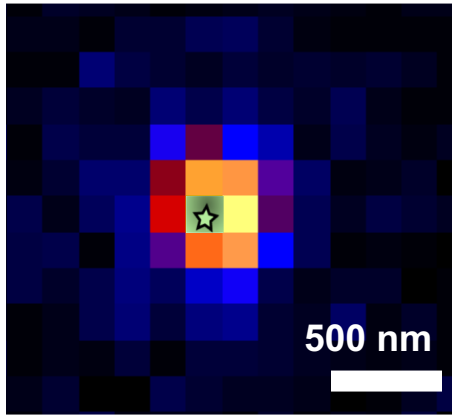

$$w_{x,y} \approx \frac{\lambda}{2NA} > 200nm$$

$$w_z \approx \frac{2\lambda\eta}{(NA)^2} > 500nm$$

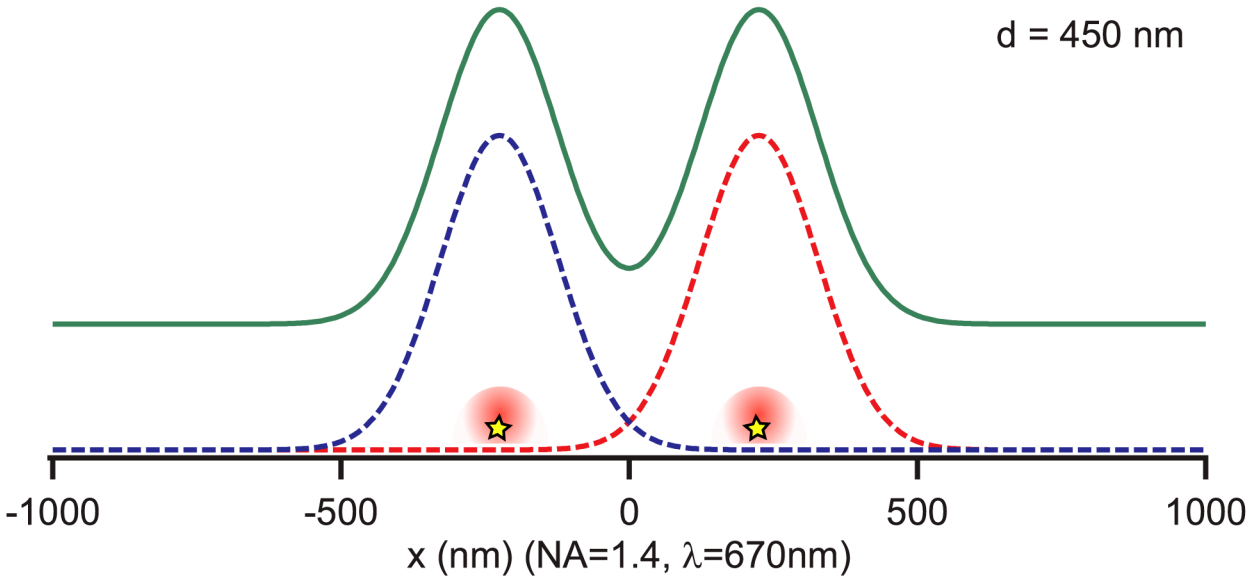

Diffraction limit

Point Spread Function (PSF)

E Abbe, Arch Mikr Anat,1873

GB Airy, Transactions of the Cambridge Philosophical Society, 1835

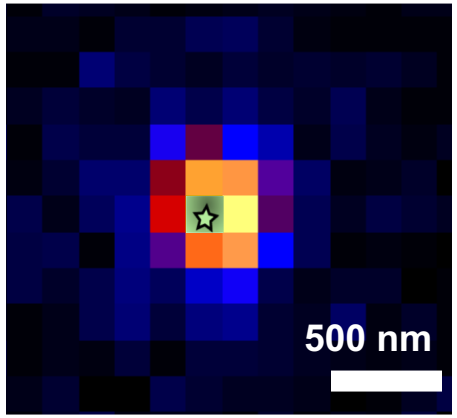

$$w_{x,y} \approx \frac{\lambda}{2NA} > 200nm$$

$$w_z \approx \frac{2\lambda\eta}{(NA)^2} > 500nm$$

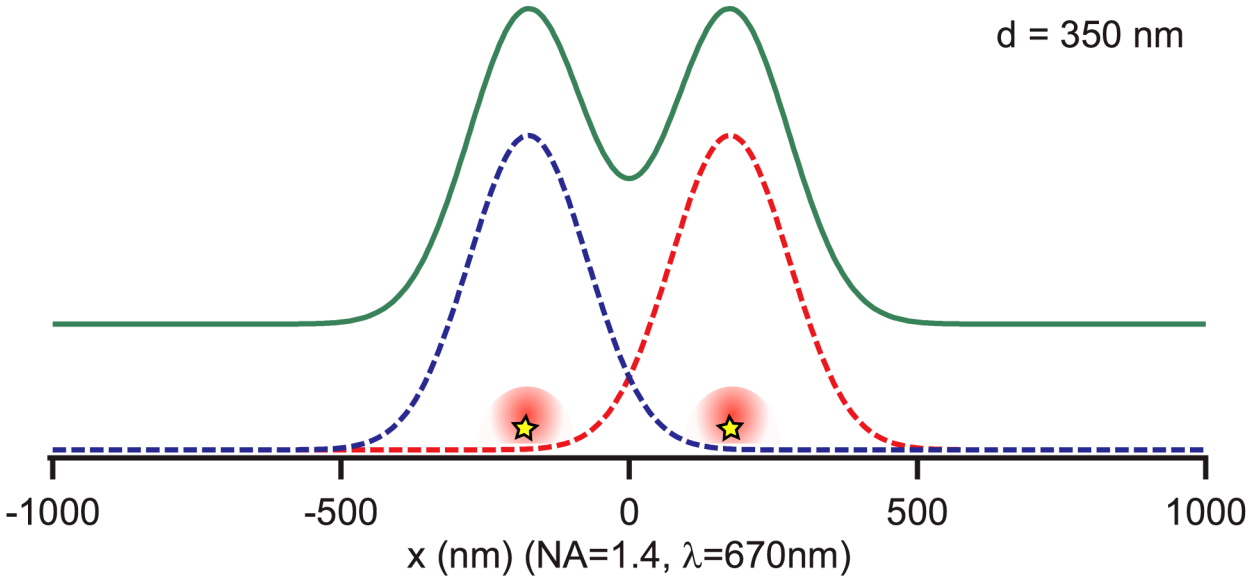

Diffraction limit

Point Spread Function (PSF)

E Abbe, Arch Mikr Anat,1873

GB Airy, Transactions of the Cambridge Philosophical Society, 1835

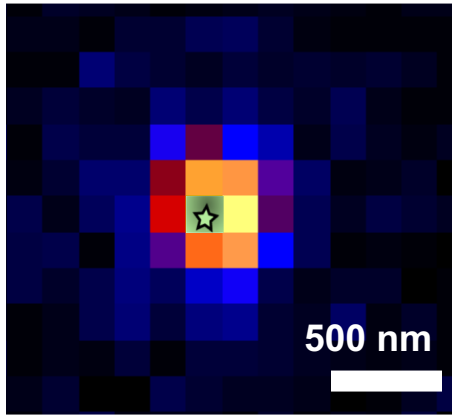

$$w_{x,y} \approx \frac{\lambda}{2NA} > 200nm$$

$$w_z \approx \frac{2\lambda\eta}{(NA)^2} > 500nm$$

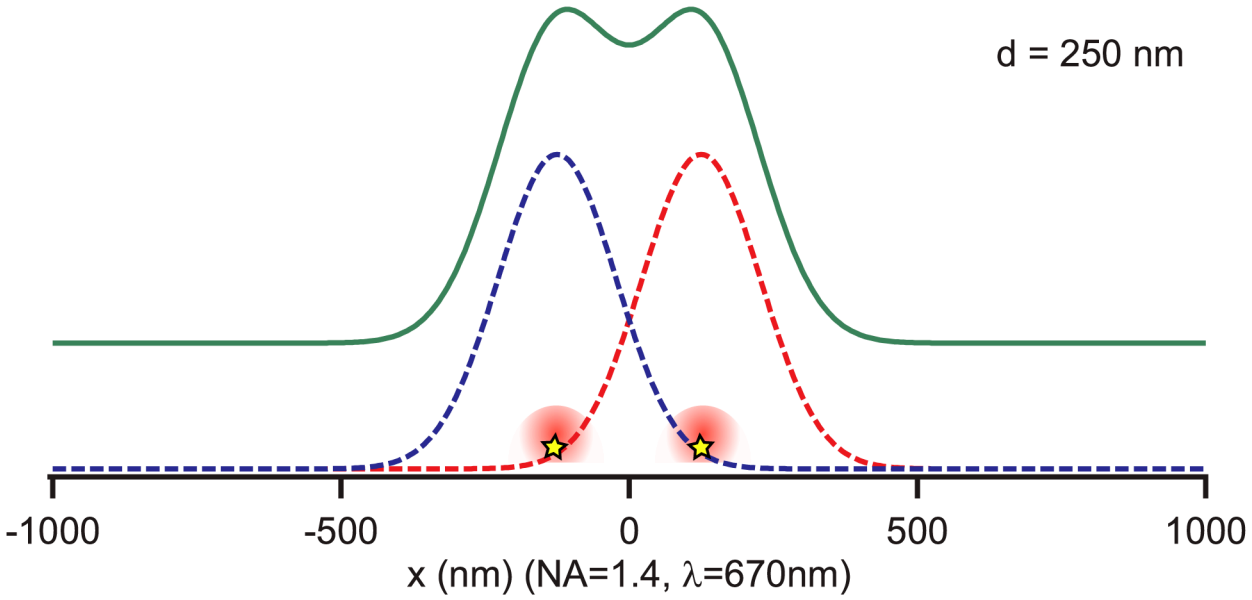

Diffraction limit

Point Spread Function (PSF)

E Abbe, Arch Mikr Anat,1873

GB Airy, Transactions of the Cambridge Philosophical Society, 1835

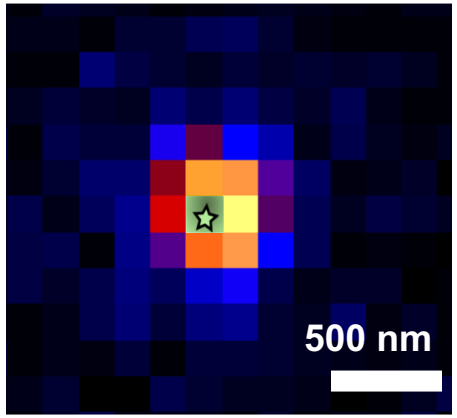

$$w_{x,y} \approx \frac{\lambda}{2NA} > 200nm$$

$$w_z \approx \frac{2\lambda\eta}{(NA)^2} > 500nm$$

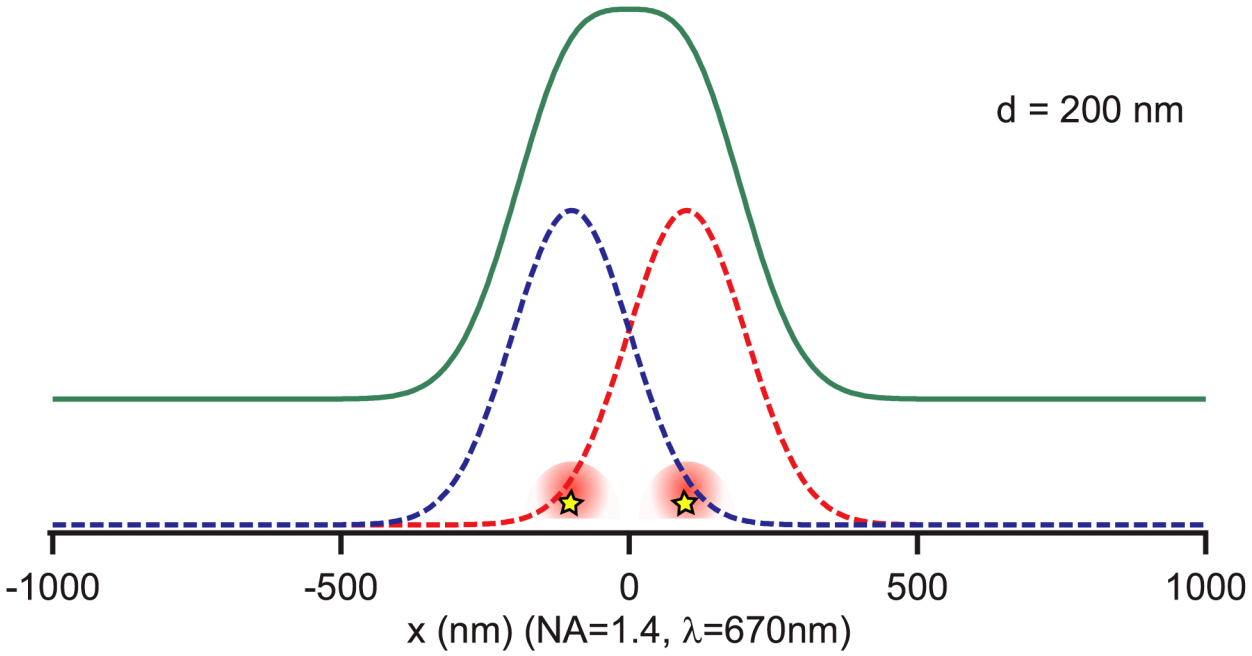

Diffraction limit

Point Spread Function (PSF)

E Abbe, Arch Mikr Anat,1873

GB Airy, Transactions of the Cambridge Philosophical Society, 1835

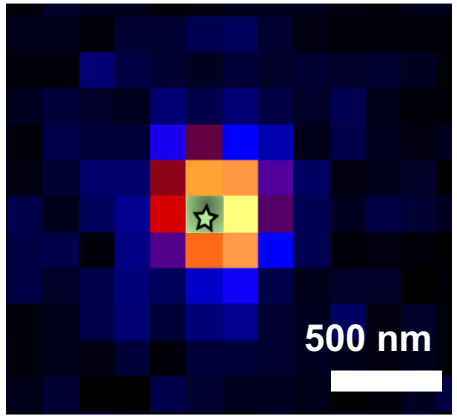

$$w_{x,y} \approx \frac{\lambda}{2NA} > 200nm$$

$$w_z \approx \frac{2\lambda\eta}{(NA)^2} > 500nm$$

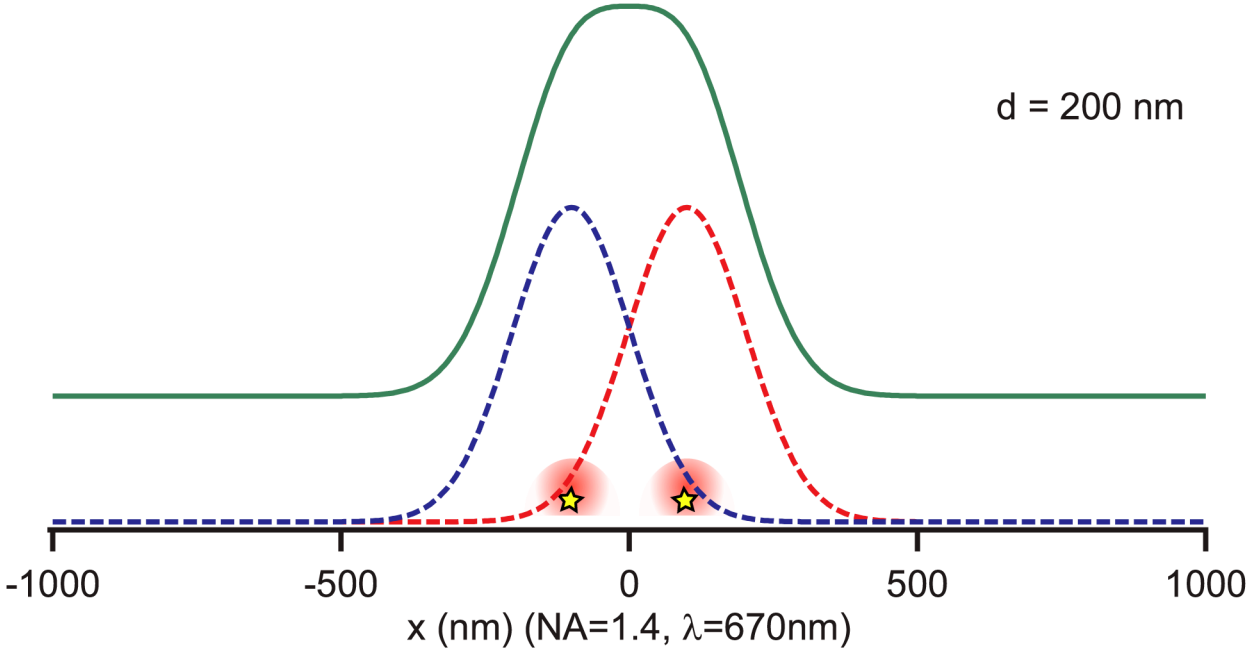

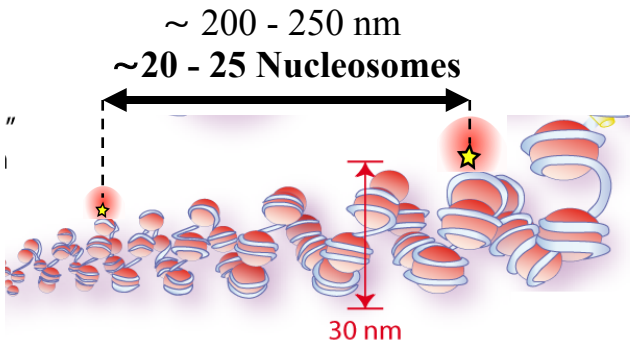

http://www.epitron.eu/index.php

Localization-based microscopy

Target structure | **Localizing activated subset of probes** | **Reconstructed image**

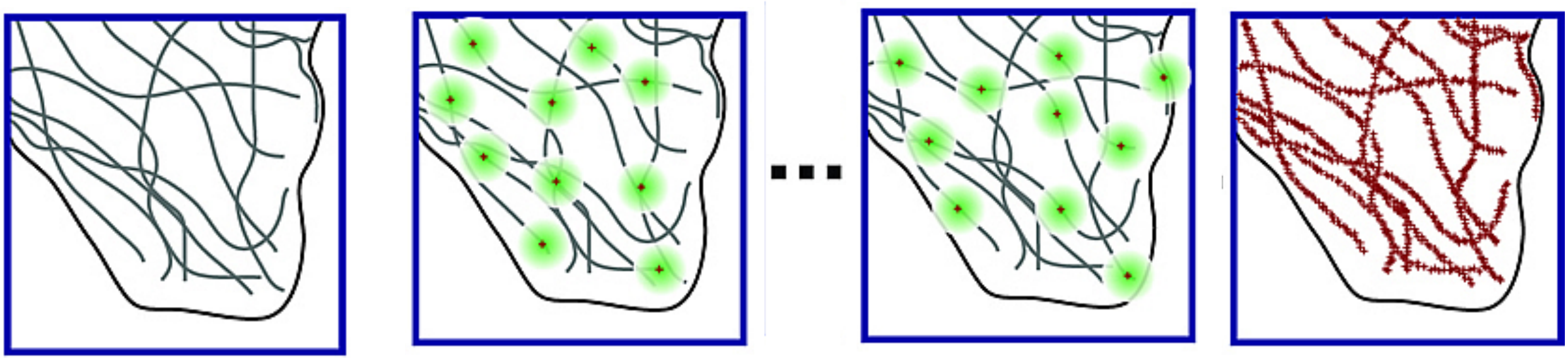

SW Hell et al., Optics letters, 1994

RM Dickson, WE Moerner et al., Nature, 1997

E Betzig et al., Science, 2006

MJ Rust, M Bates, X Zhuang, Nature methods, 2006

(~2005)

***Super-resolution microscopy**

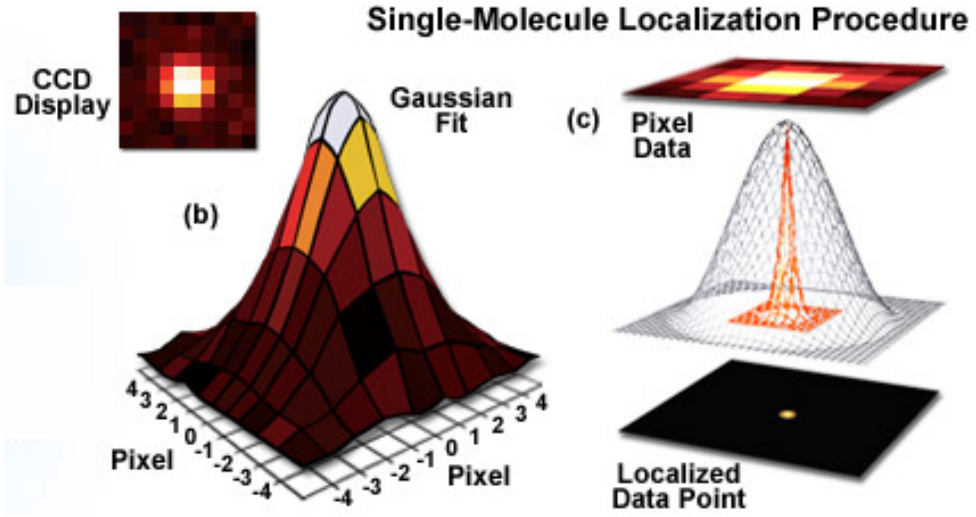

Rust et al. Nature Methods, 2006

Localization precision of ~10-50 nm

***depends on the number of collected photons**

STORM

(~2005)

Photoswitchable dyes

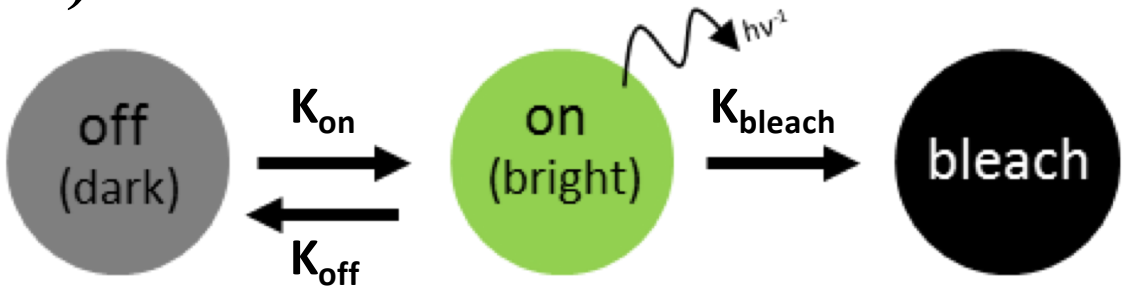

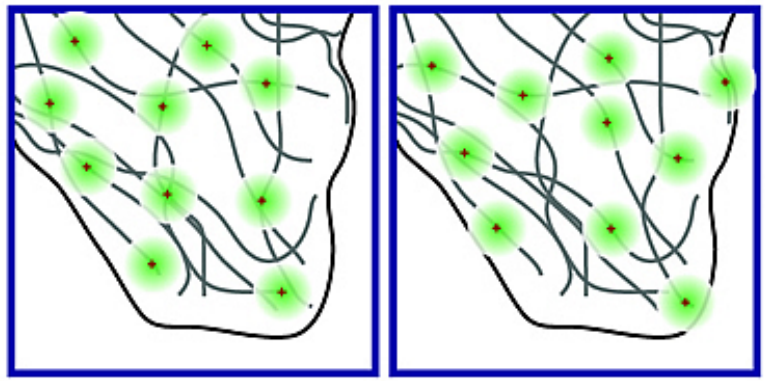

Rust et al., Nature Methods, 2006

- Medium buffer (Oxygen scavenger)
- High laser power density (~300 W/cm²)
- Activator/Reporter or Reporter

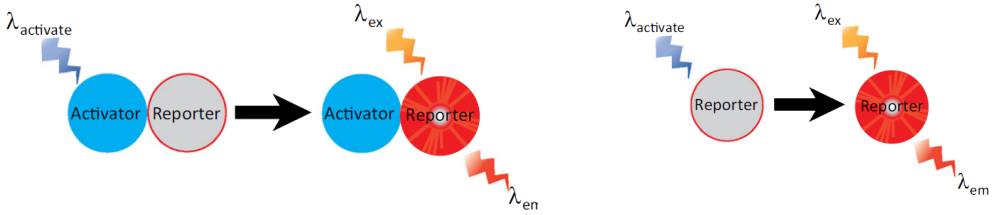

Sydor et al., Trends in Cell Biology, 2015

*The quality of the image depends on the photophysical properties of the dye

- Small ratio of: k_{on} / k_{off}
- High quantum efficiency
- Bright
- Low photobleaching

STORM: Stochastic Optical Reconstruction Microscopy

Fluorescence Microscopy: STORM & Conventional

Conventional microscopy
~250 nm resolution

Localization-based microscopy
~20 nm resolution

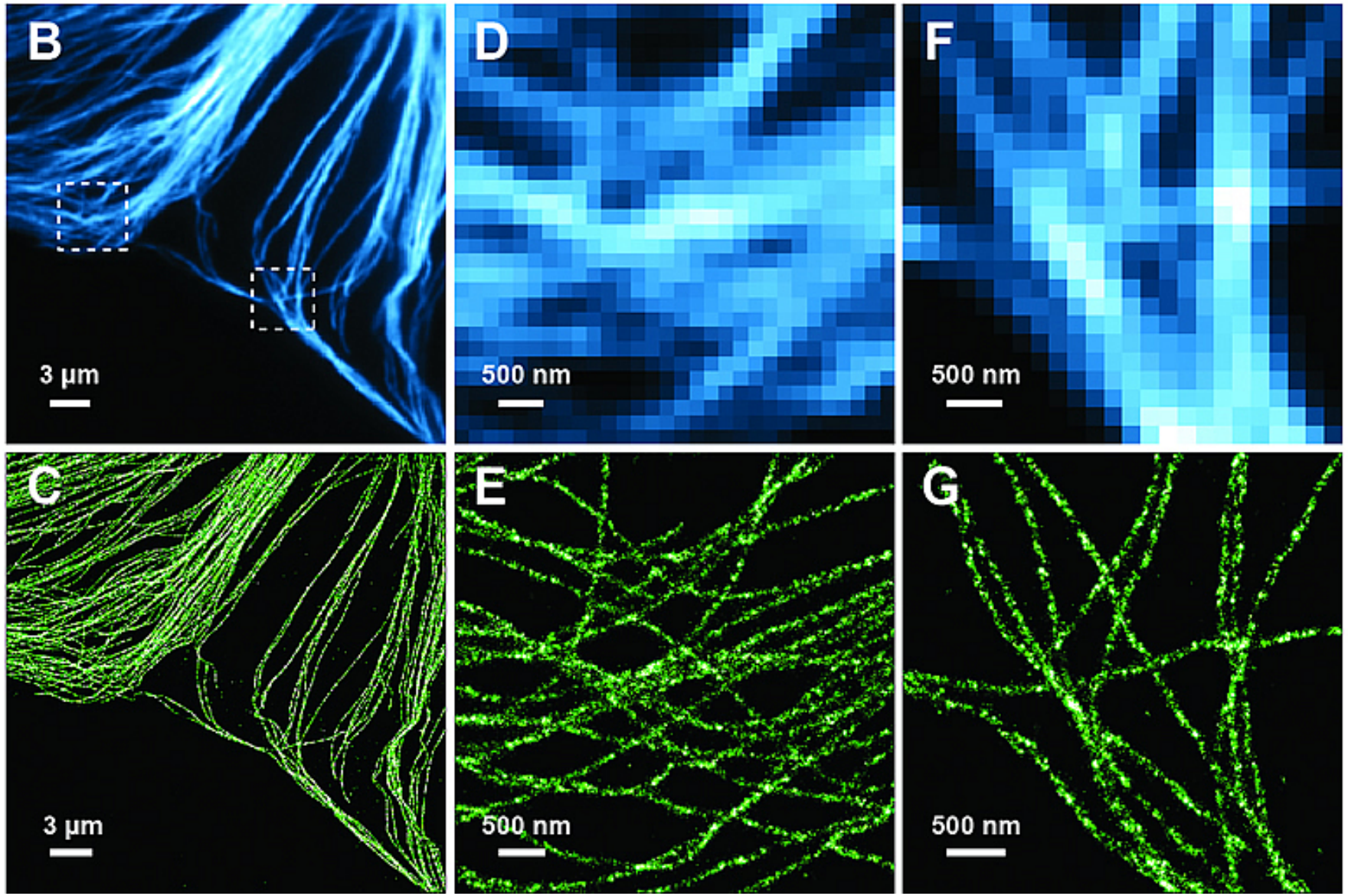

STORM: Stochastic Optical Reconstruction Microscopy

Bates et al., Science, 2007

Novel red fluorophores

red-fluorescent dyes set as benchmark

	structure	shortcomings
Atto647N	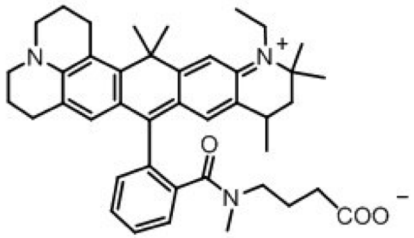	• Lipophilic character leading to background fluorescence • Two diastereomers existing (problematic for analytical methods like electrophoresis analysis)
KK114	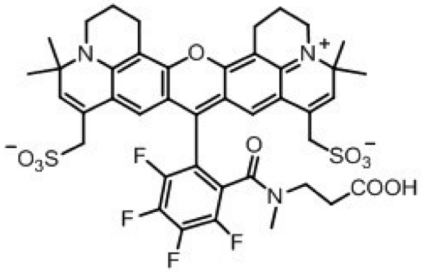	• Negative net charge of the dye (problematic for cell permeability) • Only medium stability of the NHS ester

The challenge is to design new red dyes that overcome these shortcomings and keep at the same time a good performance on

- Spectral characteristics
- Photostability
- High fluorescence quantum yields
- STED at 750 - 775nm

Wurm et al. Optical Nanoscopy 2012, 1:7

Novel red fluorophores

red-fluorescent dyes set as benchmark

	structure	shortcomings
Atto647N	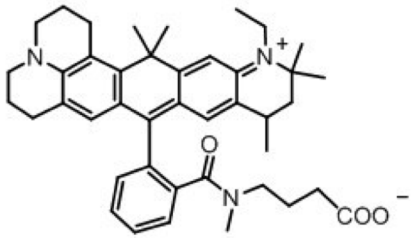	• Lipophilic character leading to background fluorescence • Two diastereomers existing (problematic for analytical methods like electrophoresis analysis)
KK114	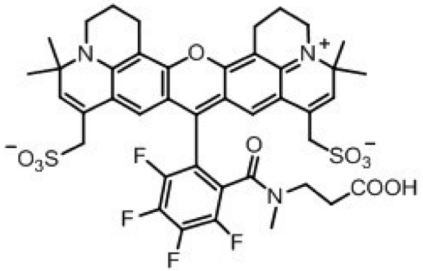	• Negative net charge of the dye (problematic for cell permeability) • Only medium stability of the NHS ester

The challenge is to design new red dyes that overcome these shortcomings and keep at the same time a good performance on

- Spectral characteristics
- Photostability
- High fluorescence quantum yields
- STED at 750 - 775nm

Wurm et al. Optical Nanoscopy 2012, 1:7

Novel red fluorophores

Four novel red-fluorescent dyes

KK1119

R: SO_3^-
X: F
n: 1

KK9046

R: OH
X: F
n: 1

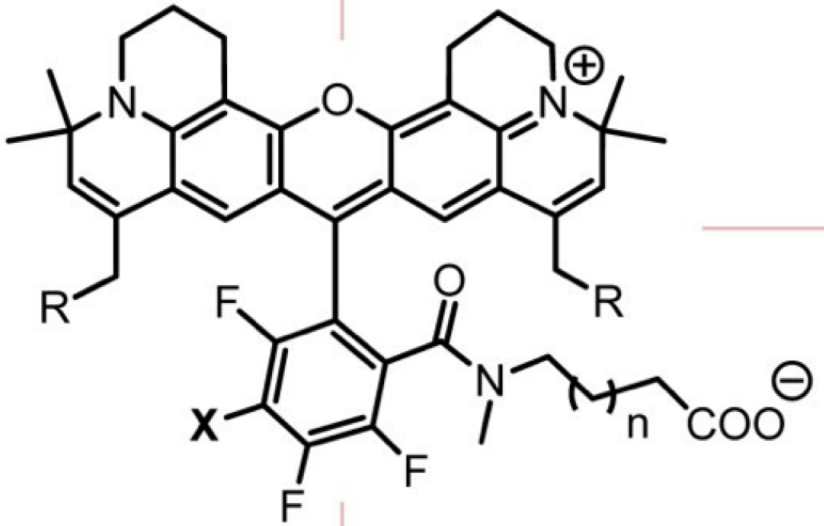

Abberior STAR635

R: OH
X: $S(CH_2)_2SO_3H$
n: 1

Abberior STAR635P

R: $OP(O)(OH)_2$
X: F
n: 1

	Absorption Max. (nm)	Emission Max. (nm)	Extinction Coefficient[a]	Net Charge[b]	NHS Stability	Fl. Quant. Yield[c]	τ_{FL} (ns)[c]	τ_{FL} (ns)[d]	Solubility[e] aq. buffer
Atto647N	644	669	1.5	+1	good	51 %	3.4	1.2	low
KK114	637	660	0.9	-1	moderate	53 %	3.6	3.6	excellent
KK1119	637	660	0.9	-1	good	55 %	3.7	1.2	excellent
KK9046	632	654	0.9	+1	good	45 %	3.6	1.8	moderate
STAR635	634	654	0.6	0	very good	51 %	3.7	2.8	good
STAR635P	635	655	0.8	-3	good	55 %	3.6	3.3	good

Wurm et al. Optical Nanoscopy 2012, 1:7

Novel red fluorophores

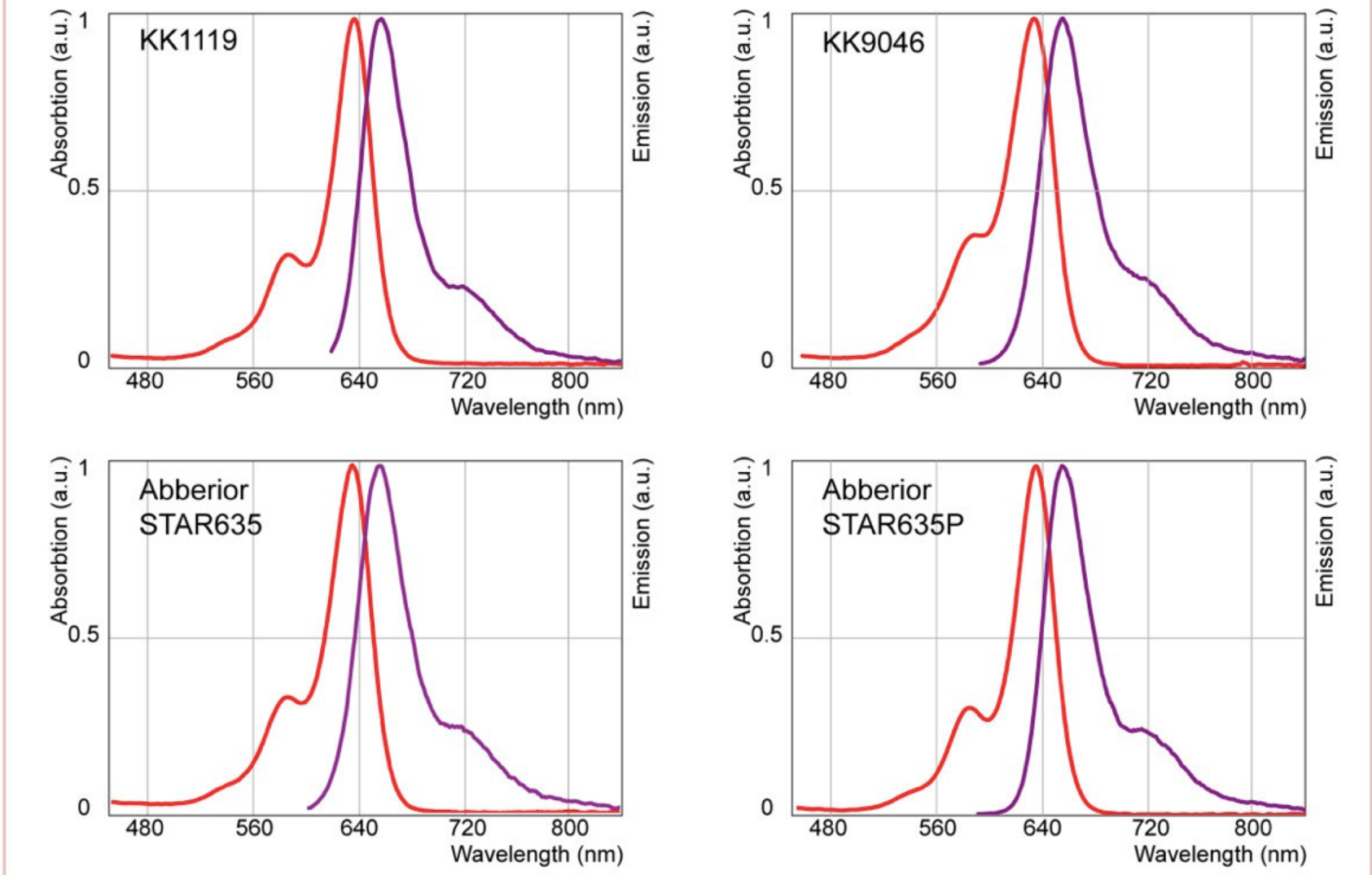

[a] x (10^{-5} L x mol^{-1} x cm^{-1}) [b] of dye residue in conjugates [c] in aq. solution [d] in cell samples [e] pH ≥7

Wurm et al. Optical Nanoscopy 2012, 1:7

STED microscopy

Figure 26. Principle of stimulated emission depletion (STED) microscopy. (**A**) STED is based on shrinking the excitation focal spot by depleting the outer excited state fluorochromes through stimulated emission with a doughnut-shaped STED beam of red-shifted and Δt time-shifted light (**B**). In essence the excitation PSF is combined with the PSF of the STED depletion laser (**B**) to produce a resultant PSF that is smaller than the diffraction limit of light. (**C**) Ultra-high resolution nanopattern distribution of the antibody-tagged SNARE protein SNAP-25 on the plasma membrane of a mammalian cell imaged with confocal and STED microscopy. The encircled areas show linearly deconvolved data. STED microscopy provides a substantial leap forward in the imaging of protein self-assembly; here it reveals for the first time that SNAP-25 is ordered in clusters of <60 nm average size. Part C adapted from [288]. © 2006 IOP Publishing Ltd.

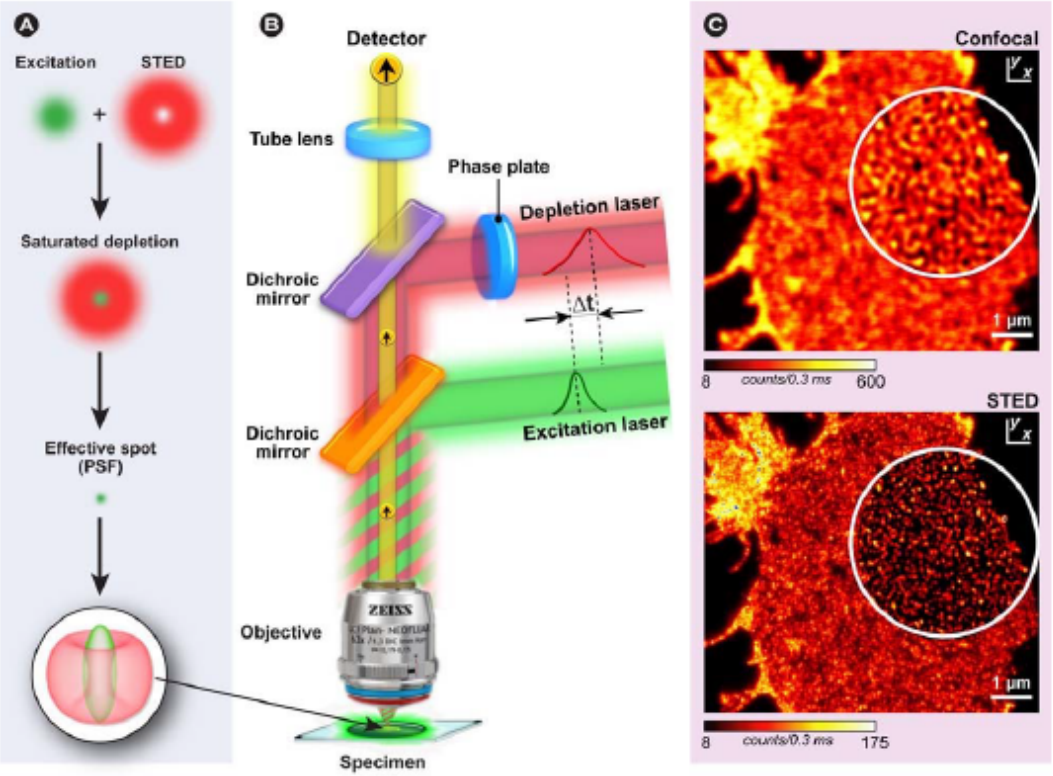

HC Ishikawa-Ankerhold et al. Molecules 2012, 17.

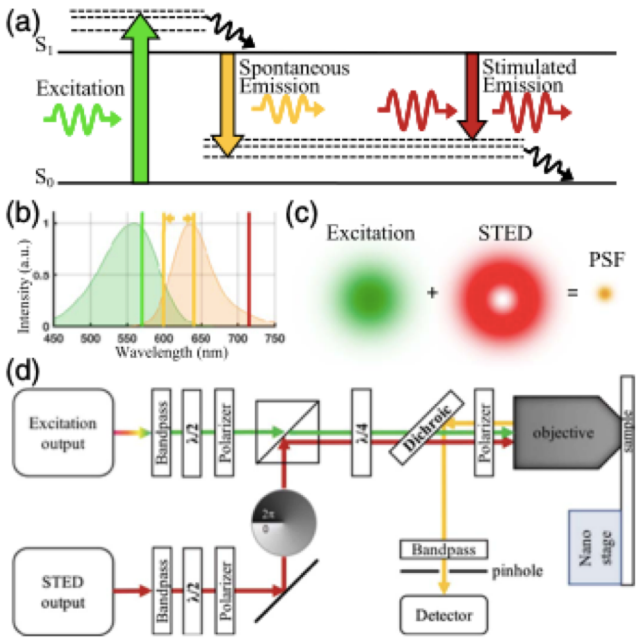

Fig. 1. Principles and implementation of STED polarizing microscopy (STED-PM). (a) Diagram illustrating the photophysical processes of fluorophores, including excitation, spontaneous emission, and stimulated emission. (b) Absorption and fluorescence spectra of Nile Red and the wavelengths and their ranges used in this work for excitation (570 nm), fluorescence detection (600–640 nm, as marked by orange arrows), and STED (715 nm). (c) Super-resolution PSF obtained by co-locating the donut-shaped STED beam and diffraction-limited excitation beam. (d) Simplified schematic of a STED polarizing microscope. A polarizer placed in an optical path right before the epi-detection objective enables polarized imaging and ensuing $\boldsymbol{n}(\boldsymbol{r})$ reconstruction based on polarization-dependent fluorescence textures. The laser pulse duration is ≈100 ps, and the repetition rate is 20 MHz.

S-H B. Tai and I.I. Smalyukh. Opt Lett 2018, 20.

Novel red fluorophores

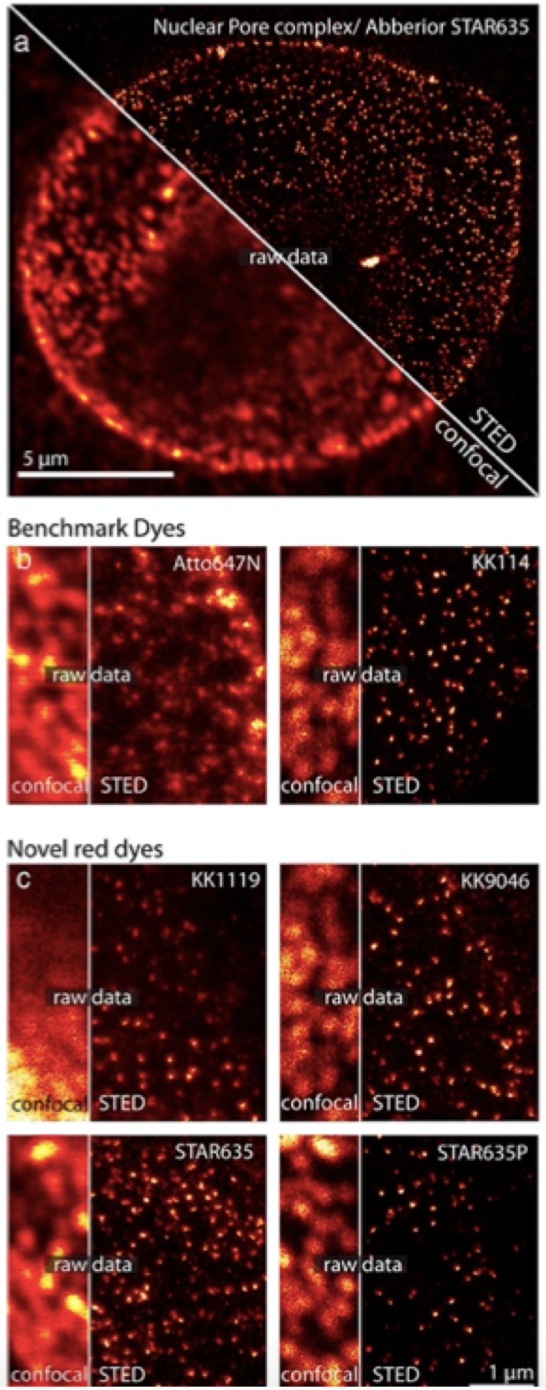

Figure 3 Comparison of the performance of the novel red dyes with the benchmark dyes Atto647N and KK114. (**a**) Overview image of the nucleus of a fixed PtK2 cell showing the Nup153 subunit of the nuclear pore complex immunolabeled with the different dyes coupled to secondary antibodies. Confocal microscopy (left) fails to discriminate individual nuclear pore complexes, whereas STED microscopy (right) identifies essentially each individual complex. (**b**) Comparison of confocal and STED recordings of the benchmark dyes Atto647N and KK114. Similar comparison between the novel red dyes in (**c**). Only subdiffraction resolution microscopy enables the accurate size determination (between 40 and 60 nm) of the labeled structures. The novel dye conjugates KK1119, KK9046, STAR635 and STAR635P display superior contrast and less background labeling than Atto647N. All data is raw.

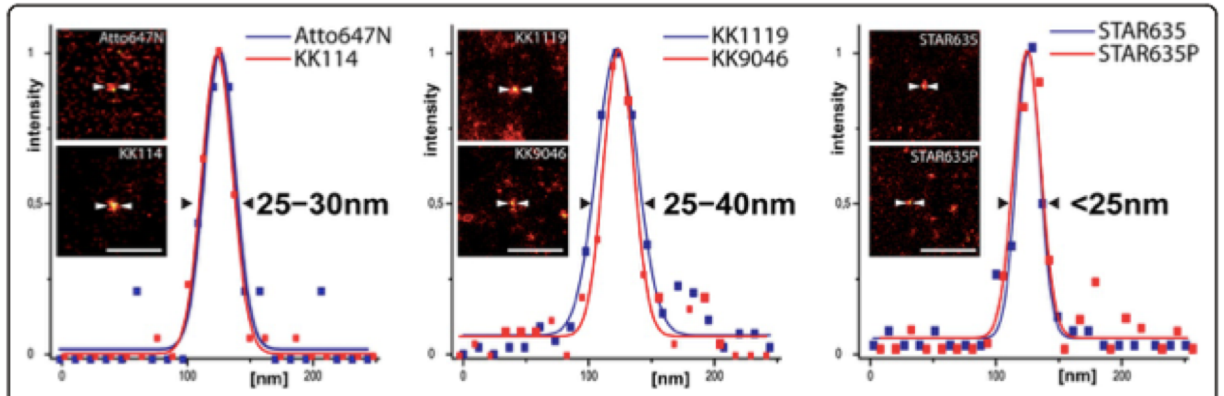

Figure 4 Spatial resolution with the benchmark dyes and the four novel red dyes in the focal plane of a STED microscope. The insert panels show the individual 'point-like' raw data spots (most likely antibody clusters) from which the shown line profiles were extracted, indicating the spatial resolution in the focal plane. The solid lines represent optimal Gaussian fit curves. The novel STAR dyes provides a focal plane resolution of <25 nm (in raw data). Scale bars, 500 nm.

Wurm et al. Optical Nanoscopy 2012, 1:7

Novel red fluorophores

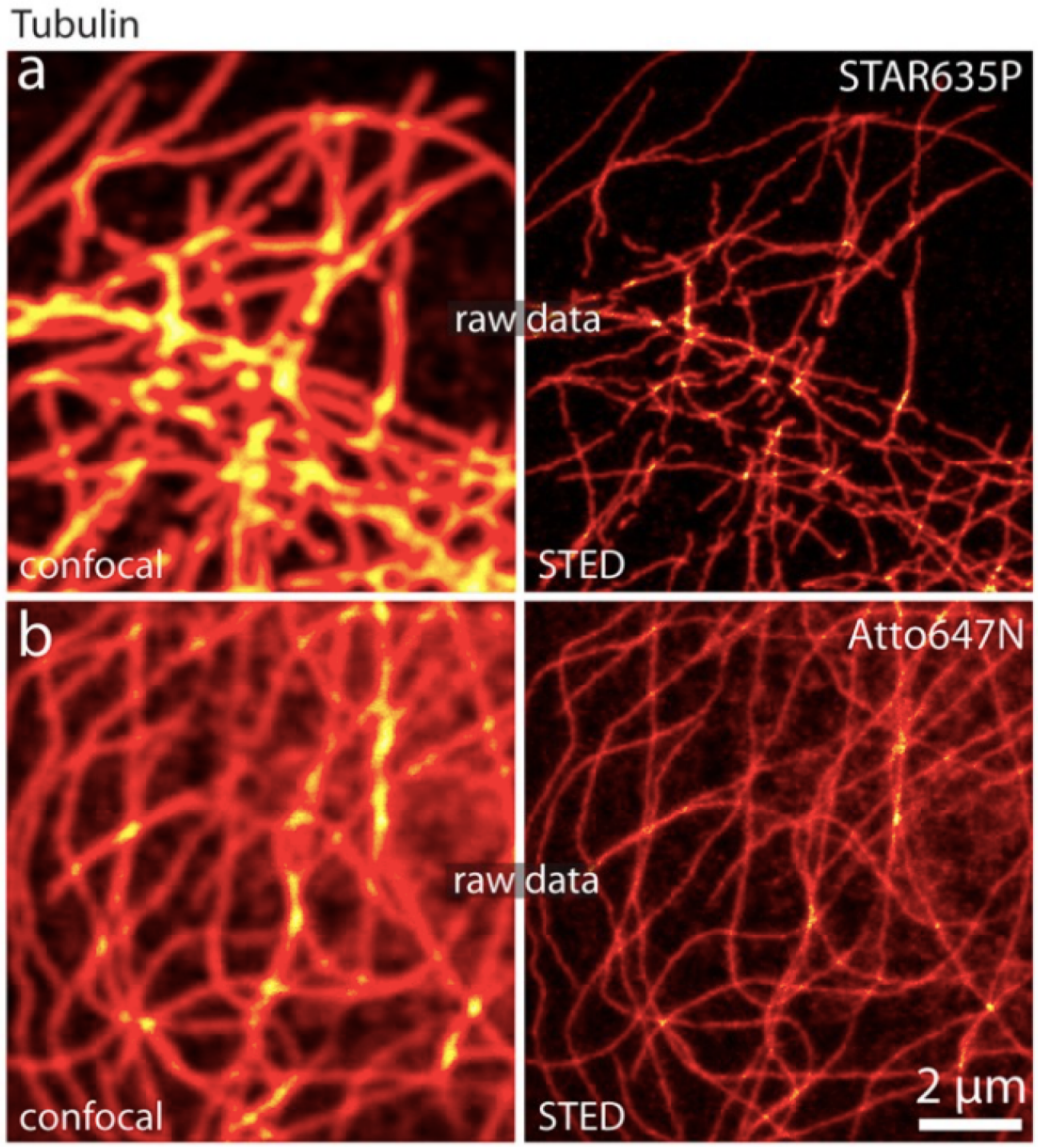

Comparison of the novel dye STAR635P (a) and the benchmark dye Atto647N. (**b**) The tubulin cytoskeleton was immunolabeled in fixed PtK2 cells and imaging of the same area in

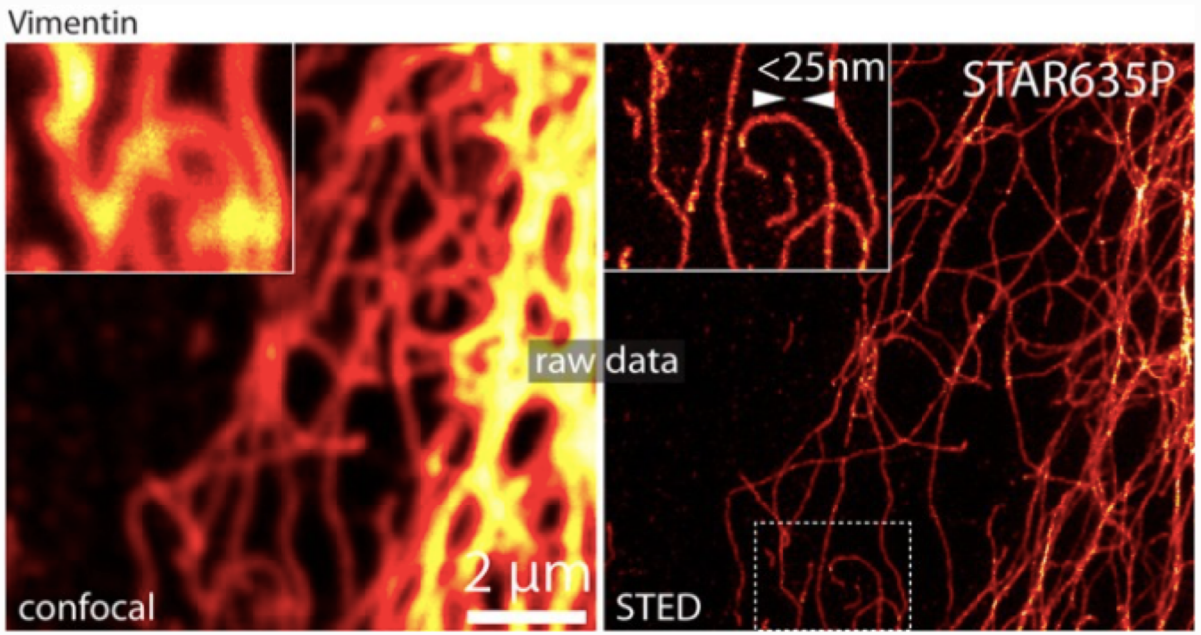

Resolution gain by STED over confocal microscopy in raw data. Confocal (left) and STED (right) imaging of Abberior STAR635P labeled Vimentin. Note the optical resolution <25 nm identified with an individual antibody cluster in the STED image (arrows in the inset).

Wurm et al. Optical Nanoscopy 2012, 1:7

FRET microscopy

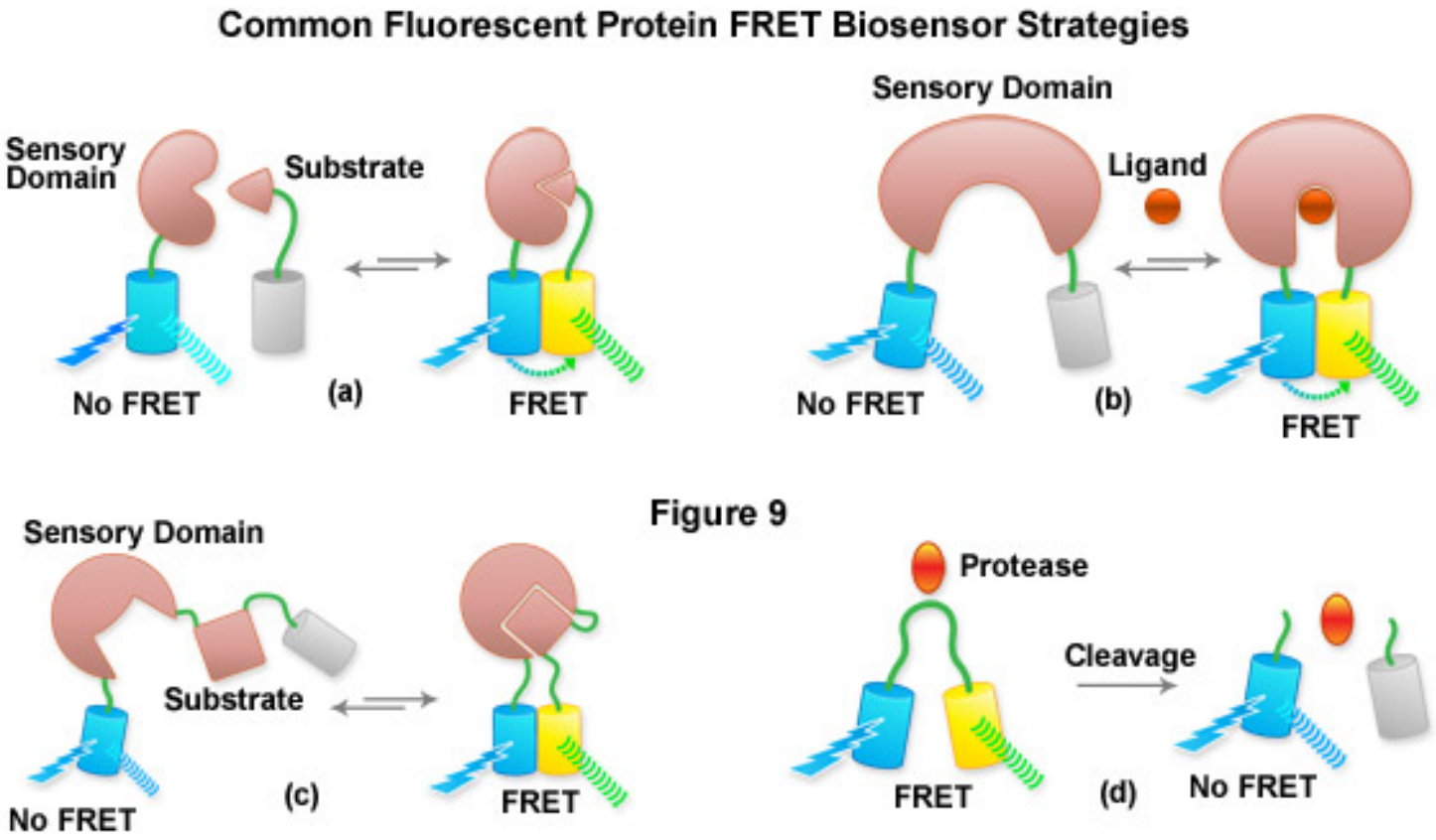

Förster Resonance Energy Transfer

FRET microscopy

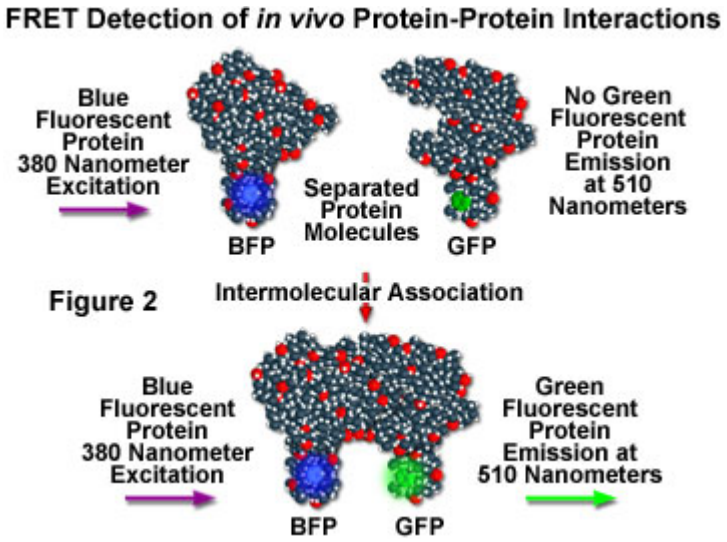

Figure 2

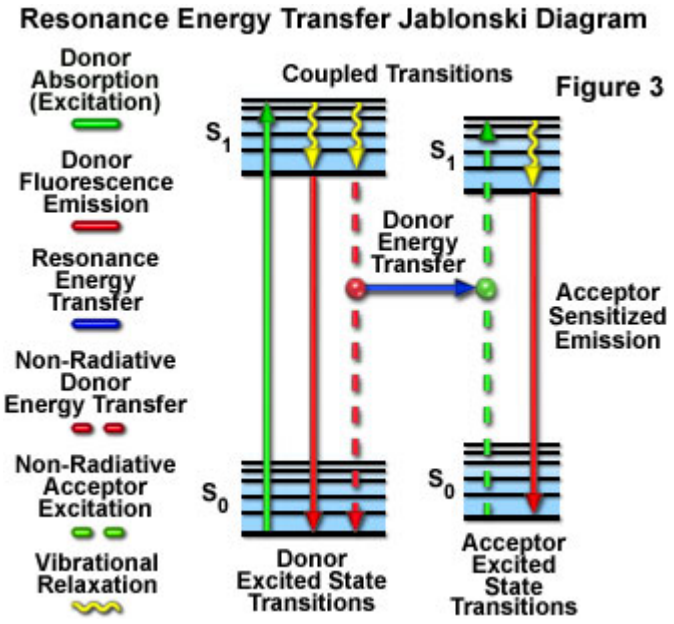

Figure 3

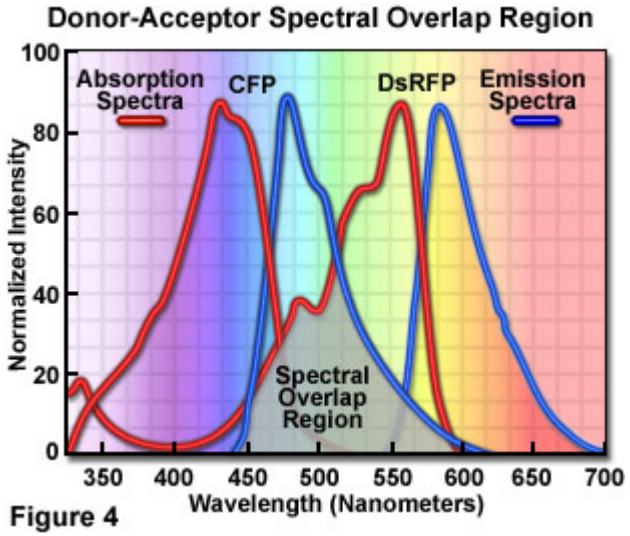

Figure 4

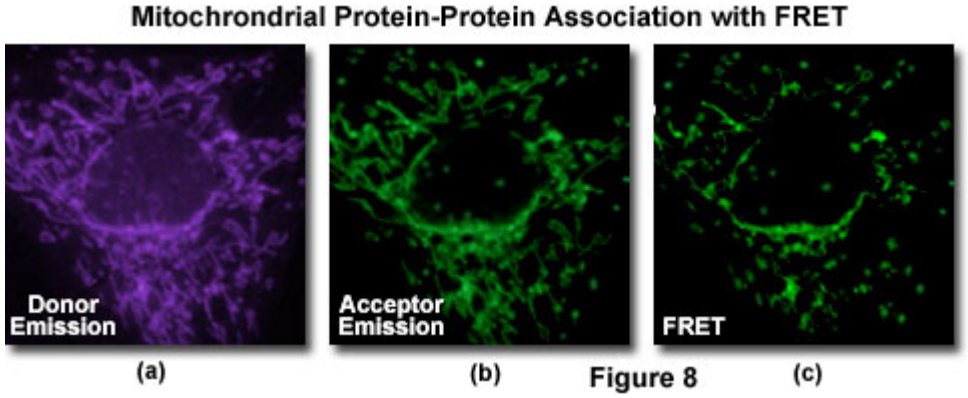

Figure 8

https://www.olympus-lifescience.com/en/microscope-resource/primer/techniques/fluorescence/fret

FRET microscopy

Figure 23. *In vivo* multiphoton FLIM-FRET measurements. Living HeLa cells co-expressing either unfused, free EGFP and unfused, free mCherry (**A**), or GFP-coupled directly to mCherry through a 17-amino-acid linker (**B**), or GFP-coupled directly to mCherry through a 7-amino-acid linker (**C**) were imaged by using a multiphoton scanning microscope. For each panel, the spatial distribution of the mean fluorescence lifetime (τ_m) and of the fluorescence lifetime of the donor molecules interacting with the acceptor (τ_{DA}) is shown throughout the cells. The FRET efficiencies were calculated for each pixel from Eq. 24 × 100%. Color scale shown covers the range of E_{FRET} values from 0% to 60%. Bars, 10 μm. Adapted from [217] with permission. © 2007 John Wiley & Sons.

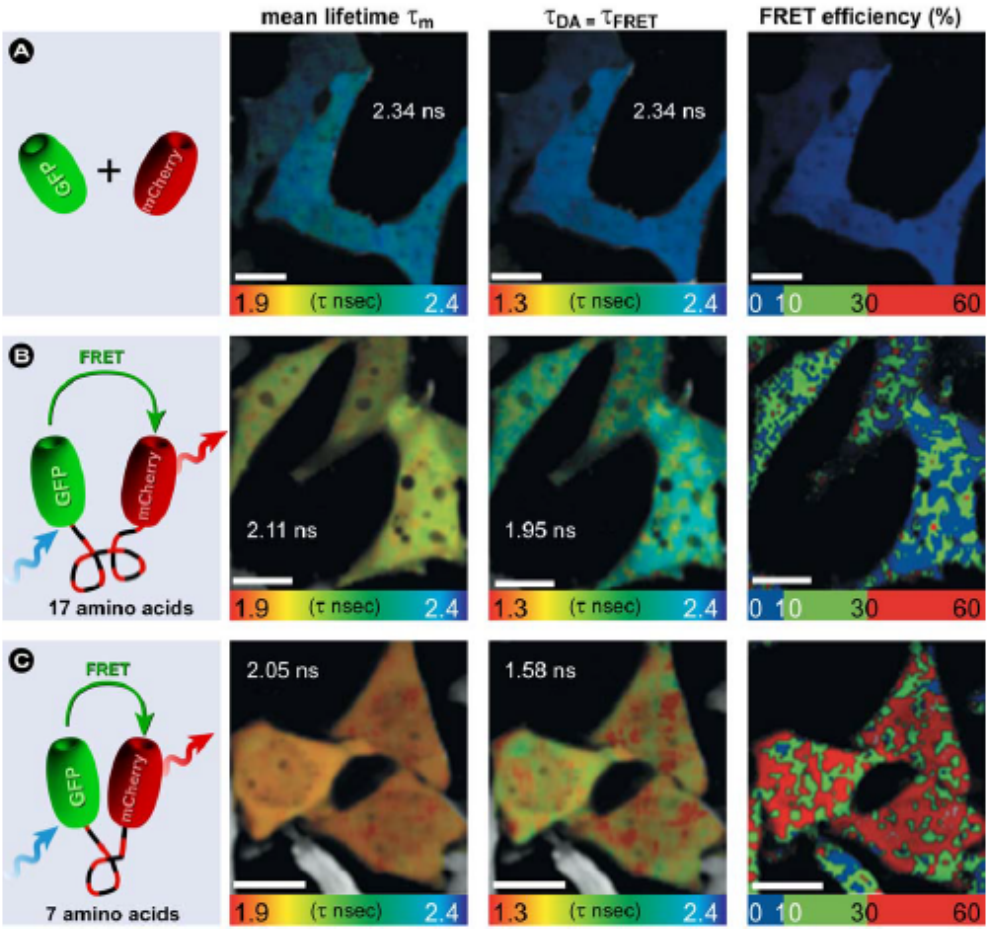

HC Ishikawa-Ankerhold et al. Molecules 2012, 17.

Diagnostic resolution – microscopy techniques

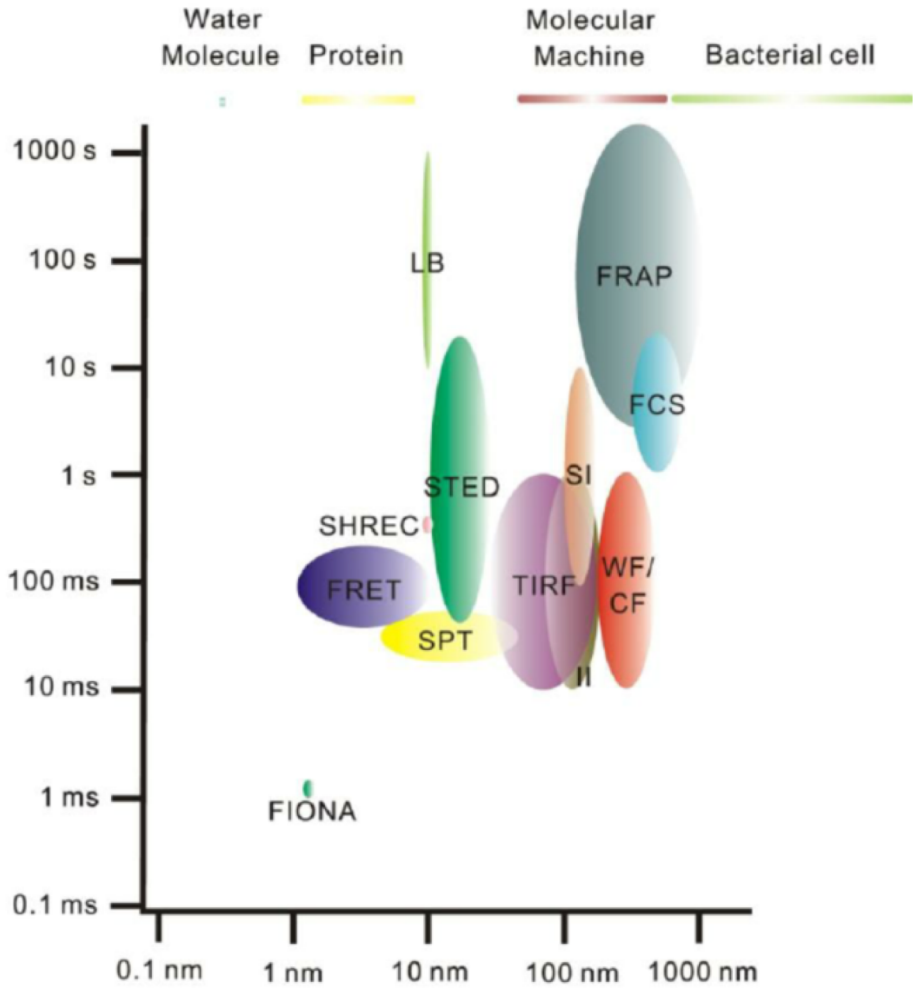

	CLSM	STED	CW-STED	3D-SIM			PALM/STORM	
~λ_{em} [nm]	460-670	670	520	620	520	460	670	520

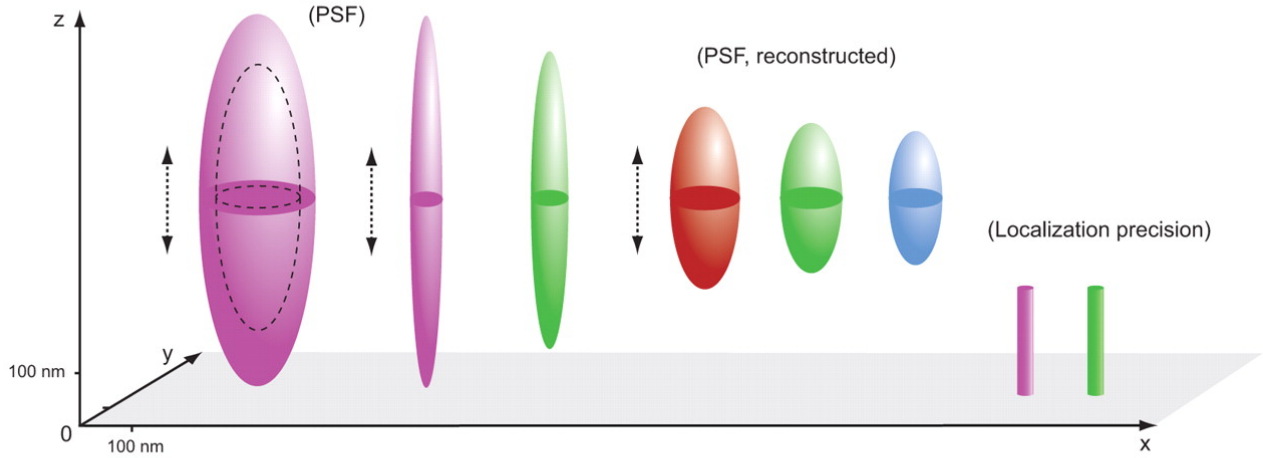

~$D_{x,y}$ [nm]	180-250	60	70	130	110	100	30
~D_z [nm]	500-700	700	560	340	280	250	140 (TIRF-range)
~$V_{x,y,z}$ [*10^{-3} μm^3]	10-23	1.3	1.5	3.0	1.8	1.3	0.1

Chiu, Sheng-Wen and Leake, Mark C. Int J Mol Sci 12(4):2518-42, 2011

DNA-PAINT

(~2010) R Jungmann et al., Nano letters, 2010

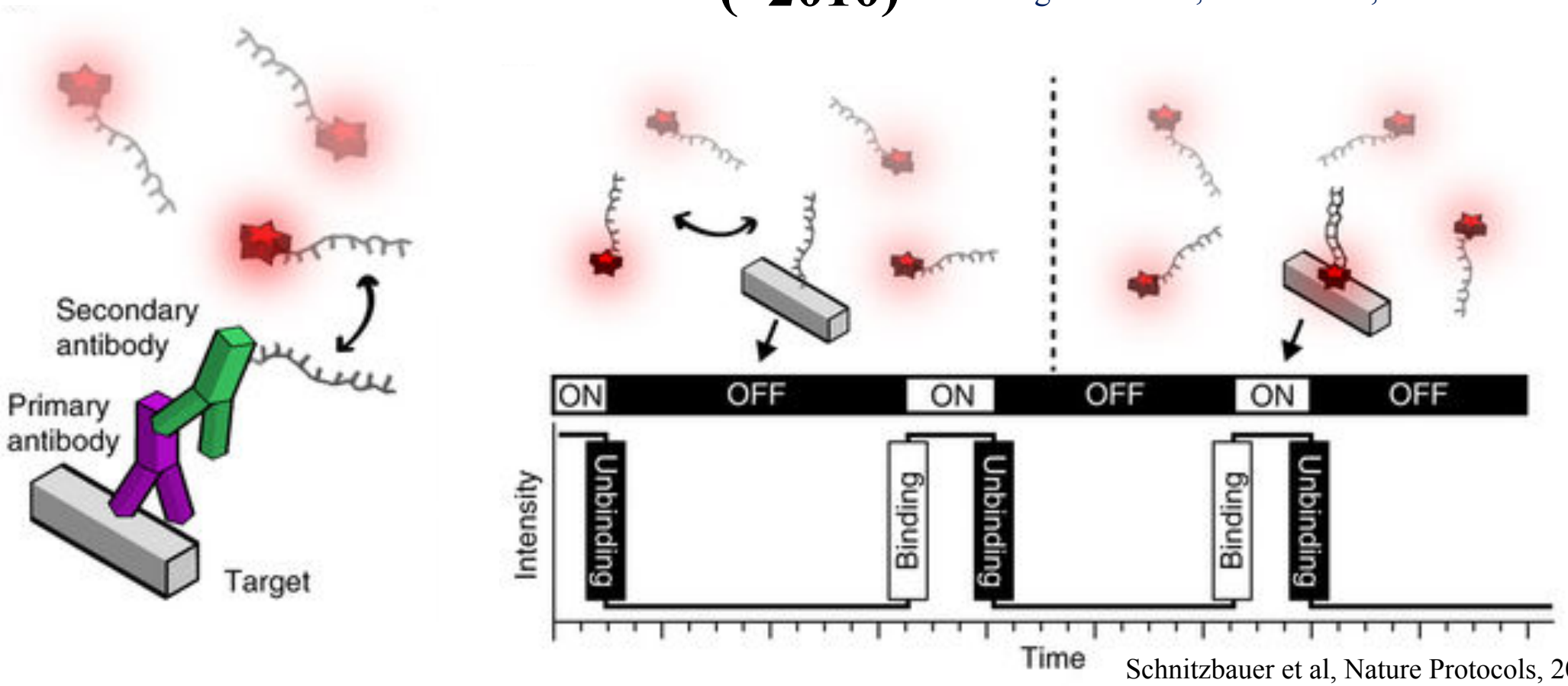

Schnitzbauer et al, Nature Protocols, 2017

- **Does not rely on fluorophore photo-physics**
- **No irreversible photo-bleaching (low laser)**
- **Image buffer not required**

- **Requires long exposure times (100 – 300 ms)**
- **Time consuming**

DNA-PAINT: DNA-based Point Accumulation for Imaging in Nanoscale Topography

DNA-PAINT

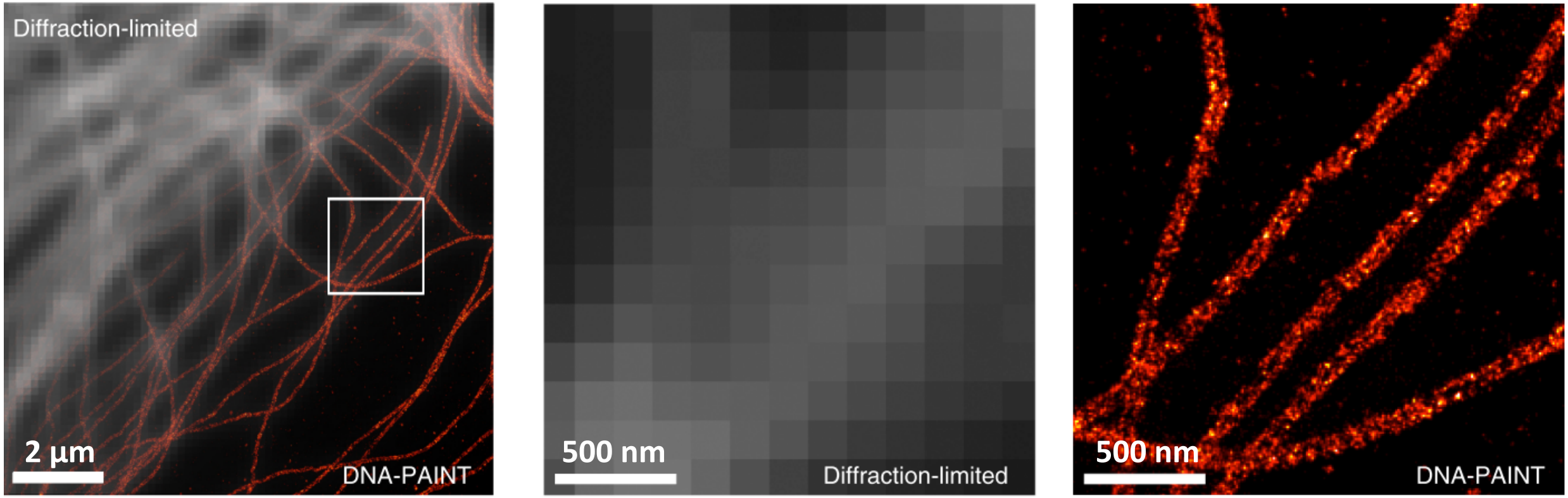

Schnitzbauer et al, Nature Protocols, 2017

DNA-PAINT: DNA-based Point Accumulation for Imaging in Nanoscale Topography